Accepted Manuscript

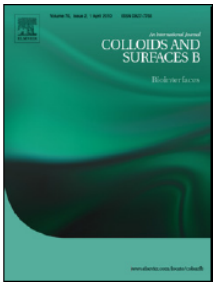

Title: Influence of hybrid polymeric nanoparticle/thermosensitive hydrogels systems on formulation tracking and *in vitro* artificial membrane permeation: a promising system for skin drug-delivery

Authors: Renato Grillo, Fabiana V. Dias, Samyr M. Querobino, Carlos Alberto-Silva, Leonardo F. Fraceto, Eneida de Paula, Daniele R. de Araujo

PII: S0927-7765(18)30747-1
DOI: https://doi.org/10.1016/j.colsurfb.2018.10.063
Reference: COLSUB 9747

To appear in: *Colloids and Surfaces B: Biointerfaces*

Received date: 18-5-2018
Revised date: 17-10-2018
Accepted date: 18-10-2018

Please cite this article as: Grillo R, Dias FV, Querobino SM, Alberto-Silva C, Fraceto LF, de Paula E, de Araujo DR, Influence of hybrid polymeric nanoparticle/thermosensitive hydrogels systems on formulation tracking and *in vitro* artificial membrane permeation: a promising system for skin drug-delivery, *Colloids and Surfaces B: Biointerfaces* (2018), https://doi.org/10.1016/j.colsurfb.2018.10.063

Influence of hybrid polymeric nanoparticle/thermosensitive hydrogels systems on formulation tracking and *in vitro* artificial membrane permeation: a promising system for skin drug-delivery

Renato Grillo [a*], Fabiana V. Dias [b], Samyr M. Querobino [b], Carlos Alberto-Silva [b], Leonardo F. Fraceto [c], Eneida de Paula [d] and Daniele R. de Araujo [b*]

[a] São Paulo State University (UNESP), Department of Physics and Chemistry, School of Engineering, Ilha Solteira, SP, Brazil;
[b] Human and Natural Sciences Center, Federal University of ABC (UFABC), Santo André, SP, Brazil;
[c] São Paulo State University (UNESP), Department of Environmental Engineering, Sorocaba, SP, Brazil;
[d] Department of Biochemistry, Institute of Biology, UNICAMP, Campinas, Brazil.

Corresponding author: renato.grillo@unesp.br (Renato Grillo) / daniele.araujo@ufabc.edu.br (Daniele R. de Araujo)

Statistical summary: The manuscript presents 5843 words, 2 tables and 4 Figures.

Graphical abstract

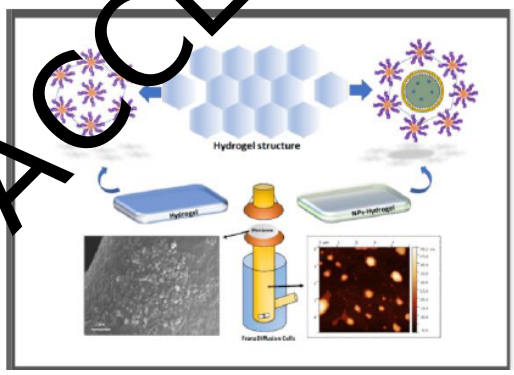

Highlights

- Characterizaon of a hybrid polymeric nanoparcle/thermosensive hydrogel system.
- NPs-hydrogel resulted in lower permeated BZC compared to the plain hydrogel.
- BZC:NPs permeated through the arcial membrane Strat-M ®.
- Development of a promising skin drug-delivery system for local anesthec benzocaine.

ABSTRACT

In recent years, the development of hybrid drug delivery systems, such as hydrogels and nanoparticles, has gained considerable attention as new formulations for skin-delivery. Meanwhile, transdermal diffusion synthetic membranes have been used to assess skin permeability to these systems, providing key insights into the relationships between drug and nanoformulations. In this study, benzocaine-loaded poly-ε-caprolactone nanoparticles (BZC:NPs) were synthesized, characterized and incorporated into Poloxamer 407-based hydrogel (PL407). Benzocaine (BZC) was used as a drug model since has been commonly applied as a topical pain reliever in the last years. Hence, we developed a hybrid polymeric nanoparticle/thermosensitive hydrogels system and evaluated the *in vitro* permeation of the BZC, as well as nanoformulation tracking in an artificial membrane. I*n vitro* permeation study was conducted in a vertical diffusion cell system using a Strat-M ® membrane model. BZC:NPs were prepared by coprecipitation method and their physico-chemical stability measured before incorporating into the thermosensitive hydrogel. Also, viscosity measurements and sol-gel transition temperature were performed by rheological analysis. Different techniques, including microscopy, were used to tracking the nanoparticles on both receptor medium and synthetic membranes. Results showed high BZC encapsulation efficiency into NPs (93%) and good physico-chemical stability before and after hydrogel incorporation. BZC i*n vitro* permeation kinetics from NPs-loaded Poloxamer 407-based hydrogel presented slower permeation profile compared with the BZC: Poloxamer 407-based hydrogel. Also, NPs were observed into the diffusion cells receptor compartment after the i*n vitro* permeation study. These results contribute to a better understanding the interaction between hydrogels, nanoparticles and synthetic membrane, as well as open perspectives for the development of new drug delivery systems for skin.

Keywords: Synthetic membrane, permeation study, hybrid systems, nanoparticles, hydrogels, controlled release.

INTRODUCTION

The growth of nanotechnology has created new therapeutic strategies to aid the treatment of diseases, mainly for the topical route, whose drug permeation is limited by the stratum corneum due to a highly hydrophobic and protein-rich region [1-3]. Among the technologies used, the development of biodegradable polymeric nanocarriers have been responsible for enhancing drug permeation across the skin barrier [4-11]. However, some studies described limitations for obtaining new formulations that present adequate rheological parameters (such as viscosity) associated to bioadhesive properties. In this sense, nanocarriers hybrid systems, such as polymeric nanoparticles-loaded hydrogels have been developed [12-14], promoting the permeation of active ingredient across the skin deeper layers since it mixes the mechanical properties of the hydrogel with the capacity to decrease the aggregation of nanoparticles, being additionally, capable of to modulate the release and permeation of the incorporated molecules [15, 16]. Then, it is worthy to note that the development of new hybrid systems can contribute in the nanomedicine field.

On the other hand, skin permeation models and/or mechanisms are still unclear, since different factors and conditions can interfere on analysis, such as pH, temperature, skin composition, size, concentration and loading of the nanocarriers, not to mention in the unexpected changes that may occur during inflammatory processes on the skin [5]. Nowadays, vertical diffusion cells (Franz-type) are the most used device to evaluate the permeation profile of active compounds, and *ex vivo* human or animal skins are used as membrane [17, 18]. In some cases, due the difficulty for obtaining biological membranes, related to sample variability and ethical issues, synthetic membranes have been used as *in vitro* model for bioactives permeation in order to obtain cheaper, reproducible assays and to perform studies regarding to formulations design [19].

Skin-mimetic membrane (Strat-M®, Merck Millipore, USA) is a type of artificial membrane composed of multiple layers of polyester sulfone that presents morphology similar

to human skin. Considering that, the Strat-M membrane layers have different pores (some more resistant to diffusion than others) impregnated with synthetic lipids [20]. Recently, studies have shown that Strat-M® can adequately simulate skin barrier performance and it can be used as a transdermal diffusion model for many drugs [20, 21]. However, few studies have reported the use of synthetic membranes to evaluate the drugs permeation profile from nanoparticulate skin-delivery system [22-24]. Moreover, there are no reports of the permeation studies of nanomaterials using this skin artificial model.

Although BZC has been used as a drug model, it is known that the development of new topical formulations for local anesthesia has been extensively explored in the last years [25, 26]. Thus, this study does not only focus on fate of active ingredient and polymeric nanoparticles in synthetic membrane, but also develop a promising controlled release system for local anesthetic to be applied to the skin. In this context, the purpose of this work was to develop a new hybrid system containing benzocaine (BZC)-loaded polymeric nanoparticles incorporated into poloxamer-based hydrogel, as well as to study the drug permeation in a transdermal diffusion membrane (Strat-M®). Furthermore, nanoparticles were tracked after the permeation assays by analytical techniques such as Photon Correlation Spectroscopy (PCS), Nanoparticle Tracking Analysis (NTA), Scanning Electron Microscopy (SEM) and Atomic Force Microscopy (AFM).

EXPERIMENTAL SECTION

Chemicals

Poly-ε-caprolactone (PCL, MW 80 kDa), benzocaine (BZC) and Poloxamer 407 (PL407) were purchased from Sigma-Aldrich. Strat-M® membrane was purchased from Merck (Darmstadt, Germany). Acetonitrile (HPLC grade) was obtained from J. T. Baker. Triglycerides of capric and caprylic acids (in the form of Myritol 318) were kindly provided by Cognis. Other reagents (analytical grade or better) were purchased from local suppliers.

Synthesis of polymeric nanoparticles

Polymeric nanoparticles (NPs) were synthesized according to the preformed polymer interfacial deposition method as described in our previously study [27]. This methodology

involves a mixture of two phases: an organic containing 100 mg of polymer (Poly- -caprolactone, PCL), 30 mL of organic solvent (acetone), 200 mg of oil (triglycerides of capric and caprylic acids, in the form of Miglyol 810), 40 mg of sorbitan monostearate surfactant (Span 60), and 100 mg of active ingredient (benzocaine, BZC). The aqueous phase was composed of 30 mL of a solution containing 60 mg of polysorbate 80 surfactant (Tween 80). After the dissolution of the components of both phases, the organic phase was poured into the aqueous phase under stirring. The nanoformulation was evaporated with a rotary evaporator to 10 mL, and the drug concentration was 10 mg.mL $^{-1}$. Also, the encapsulation efficiency (EE%) of the nanoparticle associated with BZC was evaluated by the ultrafiltration/centrifugation method using an analytical methodology previously validated by High Performance Liquid Chromatography (HPLC) as described in Supporting Information.

Preparation of hydrogel and incorporation of nanoparticles

Poloxamer 407 (PL407) solution (40 % w/v) was prepared in ice bath under magnetic stirring until complete dissolution, and maintained at 8 °C for future use. Afterwards, immediately the nanoparticles (plain or containing BZC) were added to the hydrogel in a 1:1 (volume ratio) in an ice bath under stirring for 30 minutes. In addition, hydrogels containing only BZC (at the same concentration added to nanoparticles suspension) were also prepared to be used as controls in the *in vitro* permeation assays. For drug content determination, hydrogels samples (0.5 mg) were homogenized in water (4.5 mL) during 24 h and analyzed by HPLC.

Physicochemical characterization of the nanoparticles and hybrid system

Photon Correlation Spectroscopy (PCS) was initially applied to determine the size distribution and polydispersity index of the nanoparticles, while the microelectrophoresis technique was used to determine its zeta potential. The nanoparticles and nanoparticles loaded hydrogel were analyzed by a ZetaSizer Nano ZS90 system (Malvern Instruments) at a fixed angle of 90 and 25 C. Also, the concentration of particles was determined by Nanoparticle Tracking Analysis (NTA), using a NanoSight LM 10 cell (green laser, 532 nm, Malvern Instruments) and a sCMOS camera, controlled by NanoSight v. 3.1 software.

Nanoparticle suspensions were diluted 1500-fold and all the analyses were performed in triplicate. In addition, the morphology and size distribution of the nanoparticles were evaluate by Scanning Electron Microscopy (SEM, EVO-LS-15, Carls Zeiss), operated at 15 kV of high voltage with a spot size between 3.0 - 4.0 and working distance (WD) of 10.0 mm. Size distribution measurement by SEM was presented using Image J program.

Furthermore, the hybrid hydrogel was analyzed by rheology (Oscillatory Rheometer Kinexus Lab, Malvern). All rheological measurements were conducted by a cone and plate geometry (cone upper geometry 4°/40 mm diameter) and the hydrogels containing BZC, NPs or BZC: nd loss moduli - 10 Hz and a 1 % stress-strain under constant temperature (32.5 °C). For temperature sweep tests, evolution of 50 °C was measured under a temperature range from 10 to 50 °C, at a heating rate of 5 °C.min^{-1}. From the obtained data, were determined also other parameters such as viscosity ( ) and sol-gel transition temperature (Tsol-gel). Rheograms were presented using the GraphPad Prism 6 program.

Transdermal diffusion assays across Strat-M® artificial membrane

Permeation kinetics assays were performed using a vertical Franz diffusion cell apparatus (Microette Plus, Hanson Research, Chatsworth, CA, USA) based on two compartments, donor (1.72 cm^2, permeation area) and receptor (7 mL), which were separated by a transdermal diffusion test model synthetic membrane (Strat-M ® membranes, 25 mm discs, Millipore Co, USA, an ultrafiltration membrane with thickness of 325 µm) [20]. Hydrogels samples (0.5 g) were placed in the donor compartment (in contact with Strat-M ® membrane). The receptor compartment was filled with 5 mM phosphate buffer with 154 mM saline solution (pH=7.0). The system was maintained under magnetic stirring (350 rpm) and temperature was 32.5 ± 0.5 °C. Aliquots were withdrawn at 0, 2, 6, 10, 15, 24, 48, 72 hours intervals, and then analyzed by HPLC. All experiments were performed in triplicate. The BZC cumulative amount permeated was expressed as µg.cm^{-2} and percentage and results plotted as a function of time (hours).

Tracking of the nanoparticles during transdermal diffusion study

The permeation of the nanoparticles across the transdermal diffusion synthetic membranes was also studied. During the permeation assays, aliquots from the receptor compartment were withdrawn at 24 and 72 hours and analyzed by PCS (ZetaSizer Nano ZS90, Malvern) and NTA (NanoSight LM 10 cell, Malvern). Also, aliquots were deposited onto silicon plates and analyzed by atomic force microscopy (AFM, Easy Scan 2 Basic BT02217, Nanosurf). AFM analyses were performed using an Easy Scan 2 Basic BT02217 atomic force microscope (Nanosurf, Switzerland), operated in non-contact mode with TapAl-G cantilevers (BudgetSensors, Bulgaria) and a scan rate of 90 Hz. The images (256 x 256 pixels) were captured in time mode and were analyzed using Gwyddion software. In addition, after the permeation study, each artificial membrane, were dried in a desiccator and the inner faces were metallized with thin layer of gold in sputter coater (Q150T Turbo-Pumped, Quorumtech) and analyzed by SEM to observe the presence of NPs on their inner surface.

Data Analysis

All the experiments were performed, at least, in triplicate. Results are presented as mean and standard deviation (S.D.). Statistical analyses were performed using GraphPad Prism 6.0 using two-

RESULTS AND DISCUSSION

Physicochemical characterization of the hybrid system

In recent years, several new drug-delivery systems consisting of polymers, lipids, and proteins are being synthesized [10]. However, the association of nanocarriers (such as polymeric nanoparticles) in PL407 hydrogels confers an increase on systems capability for modulating the release of different molecules. In addition, this hybrid systems improve the mechanical properties, colloidal stability and reduce the aggregation capacity of the nanocarriers [12-14].

In this study, poly-ε-caprolactone nanoparticles (with and without BZC) were synthesized and characterized, and subsequently added in PL407 hydrogels. Thus, the concentration of PCL nanoparticles in suspension measured by NTA was the order of 10^{12} nanoparticles.mL^{-1} and the average size measured by PCS was 262 ± 7 nm and 277 ± 3 nm

to the NPs and BZC:NPs, respectively. Also, similar size distribution profile and spherical morphology were observed from nanoparticles by SEM, and BZC:NPs may be observed in the Figure 1. In addition, polydispersity index were calculated and presented values below 0.2 and zeta potential up to -20 mV, as presented in Table 1, which indicate good stability and monodisperse nanoparticles. Moreover, the encapsulation efficiency (EE%) of the BZC to the nanoparticles was 93.3 ± 0.9 %. The high EE% is due its good affinity with the hydrophobic core of the NPs composed by Miglyol 810, as already shown in previous studies from our group [28, 29].

Table 1

Figure 1

Rheological analysis was performed for PL407 hydrogels containing BZC, NPs or BZC:
moduli and also the interference of BZC or NPs incorporation into the hydrogels viscosity ( ) and sol-gel transition temperature (Tsol-gel). Figure 2 presents rheological profiles and and Tsol-gel) for all hydrogels formulations.

All hydrogels formulations presented thermosensitive behavior. However, the incorporation of NPs and BZC shifted the sol-gel transition temperature (Tsol-gel), from 12.7 °C for PL hydrogels to 30 and 20.9 °C in the presence of NPs and BZC:NPs, respectively. Similarly, previous reports revealed changes on sol-gel transition temperature (Tsol-gel) values after the addition of drugs as salts [30, 31].

Regarding to rheological parameters, all formulations showed profiles inherent to viscoelastic materials, with higher on
of a gel structure. On the other hand, the NPs incorporation into the hydrogels reduced the and viscosity values, even after BZC encapsulation, showing an interference of NPs insertion on hydrogels structural organization. The presence of NP into

on PL micelle-micelle self-aggregation, an essential step for forming viscous-elastic hydrogels. Similar results were also reported by other authors, describing the influence of

biodegradable polymer (e.g. poly-lactic-co-glycolic acid) in different concentrations after incorporation into PL407 hydrogels rheological parameters [32]. Beside that, the size distribution and concentration of nanoparticles did not change when incorporated in the hydrogel (Figure S1 in the Supporting Information)

In addition, at 32.5 ºC after frequency variation ted stability to spreadability and a good application for skin-delivery, as observed in Figure S2 in the Supporting Information.

Figure 2

Table 2

***In vitro* model transdermal diffusion assays**

Figure 3 presents the BZC permeation profiles across artificial membrane Strat-M ®, from plain and NPs-hydrogels. All formulations were applied in infinite dose conditions and the total drug concentration was 5 % (w/v) for both hydrogels. Plain and NPs-hydrogels showed regular drug permeation during the experiment (72 h). However, NPs-hydrogels reduced the permeated BZC concentrations when compared to the plain hydrogels ($p < 0.001$). From those data, permeation parameters such as flux, permeability coefficient and lag-time were calculated, as expressed by Eq. 1:

(1)

where J (μg.cm^{-2}.h^{-1}) is the drug flux across the membrane, P (cm.h^{-1}) is the permeability coefficient and Cd is the drug concentration into the donor compartment. The flux values were calculated from the slope of the curves linear regression and lag time determined from the intercept at the time axis. As observed for the cumulative BZC permeated concentrations, drug flux and permeability coefficient values were lower for NPs-hydrogels (21.6 ± 1.8 g.cm^{2}.h^{1} and 4.32 x 10^{-3} cm.h^{-1}) than that observed for plain hydrogels (49.6 ± 2.1 g.cm^{2}.h^{1} and 9.92 x 10^{-3} cm.h^{-1}). In addition, NPs incorporation into the hydrogels also reduced the area under the curve ($ASC_{0\text{-}72h}$, 6319.7 ± 800.3), being statistically different from

BZC-hydrogels (15642.5 ± 1476.1, $p < 0.001$). On the other hand, similar results were observed for lag-time, being slightly slower after NPs incorporation (1.54 h) in comparison to plain hydrogel (1.32 h). Results obtained showed that hydrogels containing polymeric nanoparticles were able to reduce significantly ($p < 0.001$) the BZC permeation rate (154 g.cm ^{2}) when compared to plain hydrogels (346 g.cm ^{2}) which possibly can be due to the drug retention on membrane upper layers. Cumulative percentage-time profiles of BZC from plain and NPs-hydrogels across the Strat-M ® membrane can be also shown in Figure S3 in the Supporting Information, and it was observed a slow depletion of the drug from the donor compartment to the NPs-hydrogels. Hence, when compared NPs-hydrogels with plain hydrogel the drug permeation from NPs-hydrogel was reduced by more than 2.4 times.

Since BZC is a lipophilic drug (partition coefficient value of 93 ± 5, determined between dimyristoyl phosphatidylcholine liposomes and water, [33] and Strat-M ® upper layers are impregnated with lipids such as ceramides, free fatty acids, cholesterol and phospoholipids, the drug retention possibility could induce local anesthetic effect for a long period of time.

Considering that BZC permeation from plain hydrogels is faster than that for hybrid system, it would be expected that the continuous contact between NP and hydrogel could reduce the drug encapsulated amount and, at this point, the drug diffusion across the PL matrix and membrane would be faster. This factor has important implications on the final pharmaceutical formulation preparation, since the hybrid systems would be prepared just before application. However, the permeation profiles were obtained from an artificial membrane instead of full thickness skin, which limits to perform tape stripping analysis (useful for the quantification of drugs skin penetration and deposition) and the study of the drug skin biotransformation or blood supply influences. Others special points are the conservation of transepidermal water and skin hydration, described as conditions capable of increase the permeability of several molecules applied to the skin, since differences are also observed regarding to transepidermal water loss, being more pronounced in Strat-M ® [34], as well as reported by its wettability [20]. In this context, the viscosity of the hydrogels matrix could be changed, also modulating the drug permeation profiles and kinetics parameters.

Even Strat-M® artificial membranes have been extensively used as an alternative to human and animal skins, predicting transdermal diffusion of several compounds and skin-

delivery systems [20, 35, 36], correlations with human skin are related to diffusion parameters and further studies, using *ex vivo* models skin, are necessary to stablish the permeation and accumulation relationships for nanoparticulate systems. In fact, the polyolefin and polyethersulfone layers present in Strat- M® membrane mimic the epidermis and the dermis being used for evaluating diffusion processes. In this context, to better understand the whole interaction of nanoparticles with skin other kinds of membranes with different architectures is necessary to be investigated, as observed by previous studies presenting comparable results between some types of artificial membranes and skin (isopropyl myristate/silicone oil supported on polycarbonate membranes, ceramides, Strat-M® with rat, human or porcine ear skin) [37, 38]. In addition, the presence of stratum corneum in skin can also act as a physical barrier to penetration of nanoparticles. Moreover, the use of more specific techniques such as 3D confocal laser scanning microscopy [39], cutaneous microdialysis [40], Raman confocal microscopy [41], among others [18] may help to understand the permeation profile of drugs and nanoformulations in-depth region in skin tissue.

Figure 3

Tracking of the nanoparticles during transdermal diffusion study

During the permeation study aliquots were collected from the receptor compartment in specific intervals (24 and 72 hours) and analyzed by several physicochemical techniques in order to study the tracking of NPs in the Strat-M® membrane. PCS (24 hours) and NTA (72 hours) analyses showed that BZC:NPs (277 ± 3 nm) permeate through the artificial membrane (Figure 4A). By the way, a similar size distribution profile was observed when related to the control formulation (Figure S1), only the concentration of NPs that was lower than initial one ($1.3 \times 10^9 \pm 3.8 \times 10^7$ particles.mL^{-1}). Hence, hydrogel-BZC without NPs was also evaluated as control for both techniques and no size distribution profile was observed.

Additionally, aliquots from the receptor compartment (after 24 hours of permeation study) were dripped and dried into silicon grids and investigated by AFM, showing the presence of spherical nanoparticle in this compartment (Figure 4B), which is similar than

SEM images as showed in the Figure 1. BZC-Hydrogel was also studied by AFM and no nanoparticles were found (Figure S4-A in the Supporting Information). Also, after permeation studies, membranes were dried and analyzed by SEM (Figure 4C) and it was observed presence of NPs surrounding the fibers of the Strat-M ® inner face, which confirm their permeation through the membrane. On the other hand, those structures were not observed after permeation studies using the plain hydrogel (Figure S4-B in the Supporting Information).

Several reports have been used Strat-M® as skin-model membrane for diffusion studies, presenting results for hydrophilic or hydrophobic drugs in aqueous solutions or emulsions. In a recent study, Haq and colleagues, 2018 demonstrated that Strat-M ® presents, for diffusion experiments conditions [37], better correlation to human skin compared to cellulose acetate membrane [21, 42, 43].

Strat-M® is an artificial and inert membrane with a structural arragement composed of two layers of polyethersulfone (PES) and one support of polyolefin (POF) layer with thickness measuring ~ 300 µm. The PES and POF layers are increasingly porous, larger in thickness and the PES upper layers homogeneously treated with a combination of lipids such as ceramides, cholesterol, free fatty acids. In terms of hydrophobicity and layers arrengement, Strat-M® can be considered as a predictive model of diffusion, however reports in the literature did not provide precise information about their pore diameter size, since this information could be essencial to understand the modulation of nanoparticulate systems permeation, including the interactions with their components, charge and size. Then, the use of those membranes models presents a number of drawbacks, even they have wide applications for screening formulations during the early stages of the development.

Additionally, little is discussed about the NPs permeation across skin-models artificial membranes, such as Strat-M®. In fact, the presence of a tensoactive corona (for improving NPs coloidal stability properties) and the high water content into the NPs emulsion could modulate their permeation across the PES deeper layers, associated to the possible higher Strat-M® average pore diameter compared to that observed for human skin (~ 40 nm) [44].

On the other hand, results presented here are promising and contribute to a better understanding of the interaction among NPs, hydrogels and transdermal membrane models.

This study proposes that hybrid delivery-systems composed of NPs-loaded hydrogels can reach deeper layers, being a useful carrier of drugs, including local anesthetics. In addition, showed that NPs-hydrogels can be possible promising depot formulations on superficial skin layers, a useful strategy for the longer duration of action of topical local anesthetics. This fact can be attributed to the formation of a double system for the BZC controlled release, composed of a micellar hydrogel (formed by the arrangement of PEO and PPO monomers from PL 407) associated with a nanoparticulate system (PCL nanoparticles), showing a slower permeation profile when compared to plain hydrogels. Moreover, the fate of nanoparticles by different physicochemical techniques has been little explored on permeation studies throught synthetic skin-models membranes, mainly PCS and NTA, simultaneously. Those techniques are essential for characterize skin-delivery systems, since it is possible to observe the differences among several nanocarriers according to their capability to across membranes.

Figure 4

Conclusions

Poloxamer hydrogel containing benzocaine and PCL nanoparticles-loaded hydrogel were synthesized aiming to develop a new skin hybrid drug-delivery formulation, as well, to study an *in vitro* membrane permeation using a synthetic membrane. The results showed high drug encapsulation efficiency into the nanocapsules, adequate physico-chemical stability and rheological properties. Benzocaine- loaded NPs incorporated into the hydrogels exhibited slower permeation kinetics compared with plain hydrogel. Also, NPs were observed into the acceptor compartment on different periods after membrane permeation experiments, showing that those nanocarriers were able to across the Strat-M ® membranes. Those results contribute to better understanding of the interaction between hydrogels nanoparticles and transdermal diffusion synthetic membranes, as well, to develop a hybrid skin drug-delivery system capable of modulate the local anesthetic permeation rate.

Acknowledgments

The authors are grateful for financial support provided by the São Paulo State Science Foundation (FAPESP, grants (#2014/14457-5 and #2015/26189-8) and CNPq. We would also like to thank E. J. de Souza for assistance in the SEM analyses.

Support Information

Description of the analytical HPLC conditions for drug analysis and encapsulation efficiency (EE%). Figure S1 (Size distribution and particles concentration of the BZC:NPs and PL-BZC:NPs), Figure S2 (rheological analysis on a frequency range of 0.1 - 10 Hz and constant temperature), Figure S3 (Cumulative percentage-time profiles of BZC from plain and NPs-hydrogels) and Figure S4 (atomic force microscopy and scanning electron microscopy analysis of PL-BZC after 24 hours of permeation study).

Notes

The authors declare no competing financial interest.

References

[1] N.G. Kotla, B. Chandrasekar, P. Rooney, G. Sivaraman, A. Larranaga, K.V. Krishna, A. Pandit, Y. Rochev, Biomimetic Lipid-Based Nanosystems for Enhanced Dermal Delivery of Drugs and Bioactive Agents, Acs Biomater Sci Eng, 3 (2017) 1262-1272.

[2] S. Marepally, C.H.A. Boakye, P.P. Shah, J.R. Etukala, A. Vemuri, Design, Synthesis of Novel Lipids as Chemical Permeation Enhancers and Development of Nanoparticle System for Transdermal Drug Delivery (vol 8, e82581, 2013), Plos One, 9 (2014).

[3] A.Z. Alkilani, M.T. McCrudden, R.F. Donnelly, Transdermal Drug Delivery: Innovative Pharmaceutical Developments Based on Disruption of the Barrier Properties of the stratum corneum, Pharmaceutics, 7 (2015) 438-470.

[4] X.J. Cai, A. Woods, P. Mesquida, S.A. Jones, Assessing the Potential for Drug-Nanoparticle Surface Interactions To Improve Drug Penetration into the Skin, Mol Pharmaceut, 13 (2016) 1375-1384.

[5] A. Patzelt, W.C. Mak, S. Jung, F. Knorr, M.C. Meinke, H. Richter, E. Ruhl, K.Y. Cheung, N.B.N.N. Tran, J. Lademann, Do nanoparticles have a future in dermal drug delivery?, J Control Release, 246 (2017) 17[illegible]182.

[6] M. Elsabahy, K.L. Wooley, Design of polymeric nanoparticles for biomedical delivery applications, Chem Soc Rev, 41 (2012) 2545-2561.

[7] R. Alvarez-Roman, A. Naik, Y. Kalia, R.H. Guy, H. Fessi, Skin penetration and distribution of polymeric nanoparticles, J Control Release, 99 (2004) 53-62.

[8] I. Takeuchi, T. Suzuki, K. Makino, Skin permeability and transdermal delivery route of 50-nm indomethacin-loaded PLGA nanoparticles, Colloids Surf B Biointerfaces, 159 (2017) 31[illegible]-317.

[9] I. Takeuchi, T. Takeshita, T. Suzuki, K. Makino, Iontophoretic transdermal delivery using chitosan-coated PLGA nanoparticles for positively charged drugs, Colloids Surf B Biointerfaces, 160 (2017) 520-526.

[10] N. Kamaly, B. Yameen, J. Wu, O.C. Farokhzad, Degradable Controlled-Release Polymers and Polymeric Nanoparticles: Mechanisms of Controlling Drug Release, Chem Rev, 116 (2016) 2602-2663.

[11] Z. Zhang, P.C. Tsai, T. Ramezanli, B.B. Michniak-Kohn, Polymeric nanoparticles-based topical delivery systems for the treatment of dermatological diseases, Wires Nanomed Nanobi, 5 (2013) 205-218.

[12] M. Biondi, A. Borzacchiello, L. Mayol, L. Ambrosio, Nanoparticle-Integrated Hydrogels as Multifunctional Composite Materials for Biomedical Applications, Gels 1(2015) 162-178.

[13] X. Dong, C. Wei, J. Liang, T.J. Liu, D.L. Kong, F. Lv, Thermosensitive hydrogel loaded with chitosan-carbon nanotubes for near infrared light triggered drug delivery, Colloid Surface B, 154 (2017) 253-262.

[14] G. Manzi, N. Zoratto, S. Matano, R. Sabia, C. Villani, T. Coviello, P. Matricardi, C. Di Meo, "Click" hyaluronan based nanohydrogels as multifunctionalizable carriers for hydrophobic drugs, Carbohyd Polym, 174 (2017) 706-715.

[15] C. Dalwadi, G. Patel, Application of Nanohydrogels in Drug Delivery Systems: Recent Patents Review, Recent Pat Nanotech, 9 (2015) 17-25.

[16] P. Thoniyot, M.J. Tan, A.A. Karim, D.J. Young, X.J. Loh, Nanoparticle-Hydrogel Composites: Concept, Design, and Applications of These Promising, Multi-Functional Materials, Adv Sci, 2 (2015).

[17] L. Bartosova, J. Bajgar, Transdermal Drug Delivery In Vitro Using Diffusion Cells, Curr Med Chem, 19 (2012) 4671-4677.

[18] A.L.M. Ruela, A.C. Perissinato, M.E.D. Lino, P.S. Mudrik, G.R. Pereira, Evaluation of skin absorption of drugs from topical and transdermal formulations, Braz J Pharm Sci, 52 (2016) 527-542.

[19] E. Abd, S.A. Yousef, M.N. Pastore, K. Telaprolu, Y.H. Mohammed, S. Namjoshi, J.E. Grice, M.S. Roberts, Skin models for the testing of transdermal drugs, Clin Pharmacol, 8 (2016) 163-176.

[20] T. Uchida, W.R. Kadhum, S. Kanai, H. Todo, T. Oshizaka, K. Sugibayashi, Prediction of skin permeation by chemical compounds using the artificial membrane, Strat-M (TM), Eur J Pharm Sci, 67 (2015) 113-118.

[21] A. Simon, M.I. Amaro, A.M. Healy, L.M. Cabral, V.P. de Sousa, Comparative evaluation of rivastigmine permeation from a transdermal system in the Franz cell using

synthetic membranes and pig ear skin with in vivo-in vitro correlation, Int J Pharmaceut, 512 (2016) 234-241.

[22] D.E.M. Haron, Z. Chik, M.I. Noordin, Z. Mohamed, In vitro and in vivo evaluation of a novel testosterone transdermal delivery system (TTDS) using palm oil base, Iran J Basic Med Sci, 18 (2015) 1167-1175.

[23] R. Hamed, M. Basil, T. AlBaraghthi, S. Sunoqrot, O. Tarawneh, Nanoemulsion-based gel formulation of diclofenac diethylamine: design, optimization, rheological behavior and in vitro diffusion studies, Pharmaceutical Development and Technology, 21 (2016) 980-989.

[24] J.H. Kim, J.A. Ko, J.T. Kim, D.S. Cha, J.H. Cho, H.J. Park, G.H. Shin, Preparation of a Capsaicin-Loaded Nanoemulsion for Improving Skin Penetration, J Agr Food Chem, 62 (2014) 725-732.

[25] D.R. de Araujo, D.C. da Silva, R.M. Barbosa, M. Franz-Montan, C.M.S. Cereda, C. Padula, P. Santi, E. de Paula, Strategies for delivering local anesthetics to the skin: focus on liposomes, solid lipid nanoparticles, hydrogels and patches, Expert Opin Drug Del, 10 (2013) 1551-1563.

[26] E. de Paula, C.M.S. Cereda, L.F. Fraceto, D.R. de Araujo, M. Franz-Montan, G.R. Tofoli, J. Ranali, M.C. Volpato, F.C. Groppo, Micro and nanosystems for delivering local anesthetics, Expert Opin Drug Del, 9 (2012) 1505-1524.

[27] R. Grillo, N.Z.P. dos Santos, C.R. Maruyama, A.H. Rosa, R. de Lima, L.F. Fraceto, Poly(epsilon-caprolactone)nanocapsules as carrier systems for herbicides: Physico-chemical characterization and genotoxicity evaluation, J Hazard Mater, 231 (2012) 1-9.

[28] R. Grillo, N.F.S. De Melo, D.R. De Araujo, E. De Paula, N.L. Dias, A.H. Rosa, L.F. Fraceto, Validation of an HPLC Method for quantitative Determination of Benzocaine in PHBV-Microparticles and PLA-Nanoparticles, Lat Am J Pharm, 28 (2009) 393-399.

[29] N.F.S. De Melo, D.R. De Araujo, R. Grillo, C.M. Moraes, A.P. De Matos, E. de Paula, A.H. Rosa, L.F. Fraceto, Benzocaine-loaded polymeric nanocapsules: Study of the anesthetic activities, J Pharm Sci-Us, 101 (2012) 1157-1165.

[30] E.J. Ricci, M.V.L.B. Bentley, M. Farah, R.E.S. Bretas, J.M. Marchetti, Rheological characterization of Poloxamer 407 lidocaine hydrochloride gels, Eur J Pharm Sci, 17 (2002) 161-167.

(2009) 113-118.

[32] S. Salatin, J. Barar, M. Barzegar-Jalali, K. Adibkia, M. Jelvehgari, Thermosensitive in situ nanocomposite of rivastigmine hydrogen tartrate as an intranasal delivery system: Development, characterization, ex vivo permeation and cellular studies, Colloid Surface B, 159 (2017) 629-638.

[33] C.M. Avila, F. Martinez, Thermodynamics of partitioning of benzocaine in some organic solvent/buffer and liposome systems, Chem Pharm Bull, 51 (2003) 237-240.

[34] V. Carrer, B. Guzman, M. Marti, C. Alonso, L. Coderch, Lanolin-Based Synthetic Membranes as Percutaneous Absorption Models for Transdermal Drug Delivery, Pharmaceutics, 10 (2018).

[35] T. Osmalek, B. Milanowski, A. Froelich, S. Gorska, W. Bialas, M. Szybowicz, M. Kapela, Novel organogels for topical delivery of naproxen: design, physicochemical characteristics and in vitro drug permeation, Pharmaceutical Development and Technology, 22 (2017) 521-536.

[36] E.L. Tombs, V. Nikolaou, G. Nurumbetov, D.M. Haddleton, Transdermal Delivery of Ibuprofen Utilizing a Novel Solvent-Free Pressure-sensitive Adhesive (PSA): TEPIA (R) Technology, J Pharm Innov, 13 (2018) 48-57.

[37] D. Karadzovska, J.E. Riviere, Assessing vehicle effects on skin absorption using artificial membrane assays, Eur J Pharm Sci, 50 (2013) 569-576.

[38] L. Kaur, K. Singh, S. Paul, S. Singh, S. Singh, S.K. Jain, A Mechanistic Study to Determine the Structural Similarities Between Artificial Membrane Strat-M and Biological Membranes and Its Application to Carry Out Skin Permeation Study of Amphotericin B Nanoformulations, AAPS PharmSciTech, (2018).

[39] M. Singhal, S. del Rio-Sancho, K. Sonaje, Y.N. Kalia, Fractional Laser Ablation for the Cutaneous Delivery of Triamcinolone Acetonide from Cryomilled Polymeric Microparticles: Creating Intraepidermal Drug Depots, Mol Pharmaceut, 13 (2016) 500-511.

[40] P.R. Desai, P.P. Shah, R.R. Patlolla, M. Singh, Dermal Microdialysis Technique to Evaluate the Trafficking of Surface-Modified Lipid Nanoparticles upon Topical Application, Pharm Res-Dordr, 29 (2012) 2587-2600.

[41] M. Forster, M.A. Bolzinger, G. Montagnac, S. Briancon, Confocal Raman microspectroscopy of the skin, Eur J Dermatol, 21 (2011) 851-863.

[42] A. Haq, M. Dorrani, B. Goodyear, V. Joshi, B. Michniak-Kohn, Membrane properties for permeability testing: Skin versus synthetic membranes, Int J Pharmaceut, 539 (2018) 58-64.

[43] J.M. Christensen, M.C. Chuong, H. Le, L. Pham, E. Bendas, Hydrocortisone Diffusion Through Synthetic Membrane, Mouse Skin, and Epiderm Cultured Skin, Arch Drug Inf, 4 (2011) 10-21.

[44] V. Aguilella, K. Kontturi, L. Murtomaki, P. Ramirez, Estimation of the Pore-Size and Charge-Density in Human Cadaver Skin, J Control Release, 32 (1994) 249-257.

Figures Captions

Figure 1. Scanning electron microscopy of the BZC:NPs formulation: A) 10,000x magnification, B) 30,000x magnification and c) Percentage size distribution of the nanoparticles (n= 565 particles).

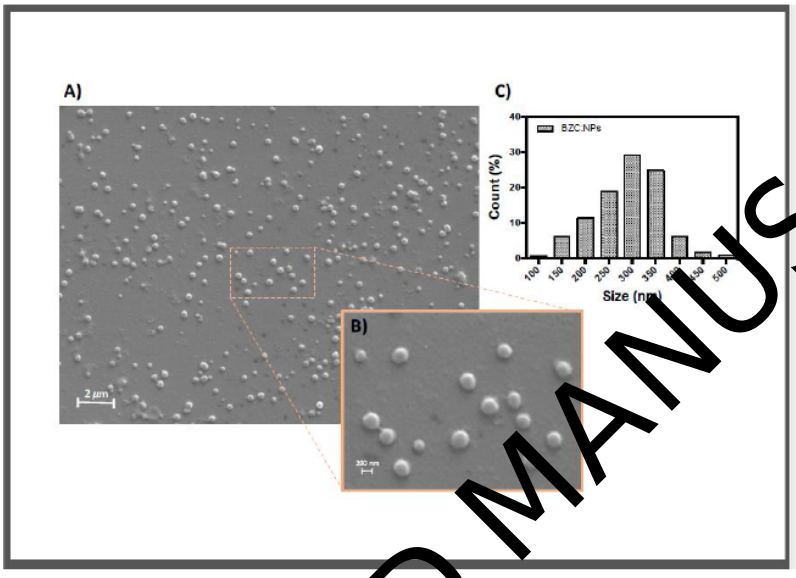

Figure 2. Rheological analysis of PL407 hydrogels (30 % w/v) containing BZC, NPs, or BZC:NPs at different temperatures. A) Hydrogel, B) Hydrogel + NPs, C) Hydrogel + BZC:NPs and D) Hydrogel + BZC.

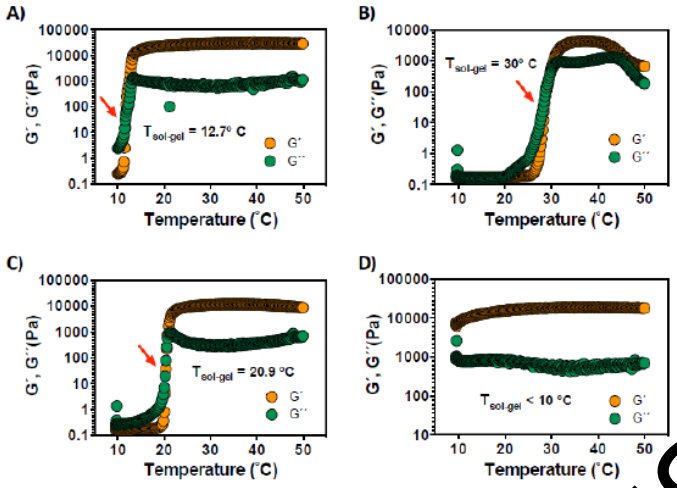

Figure 3. Permeation profiles of BZC from plain and NPs-hydrogels across the Strat-M ® membrane (mean ± SD, n = 3/formulation) using a vertical Franz diffusion cell apparatus. Hydrogels samples (0.5 g) were placed in the donor compartment and the receptor compartment was filled with phosphate buffer (pH = 7.0). The system was maintained under magnetic stirring (350 rpm) and temperature was 32 °C within 72 hours.

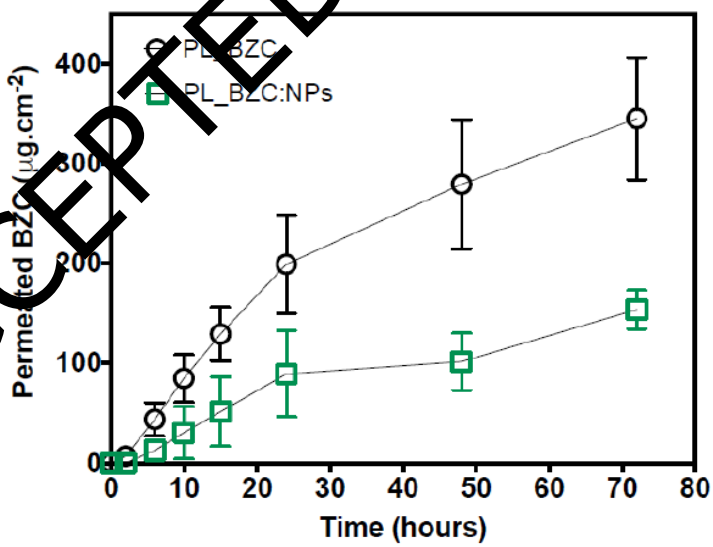

Figure 4. Tracking of the BZC:NPs in synthetic membrane (Strat-M®) after the hybrid hydrogel aplication in Strat-M® membrane: A) Size distribution profile of the BZC:NPs nanoformulation after 24 hours by DLS and after 72 hours by NTA; B) Atomic force microscopy and of the dry membrane after permeation study and C) Scanning electron microscopy of inner side of the membrane after 72 hours of permeation 5000x magnification and 20,000x magnification.

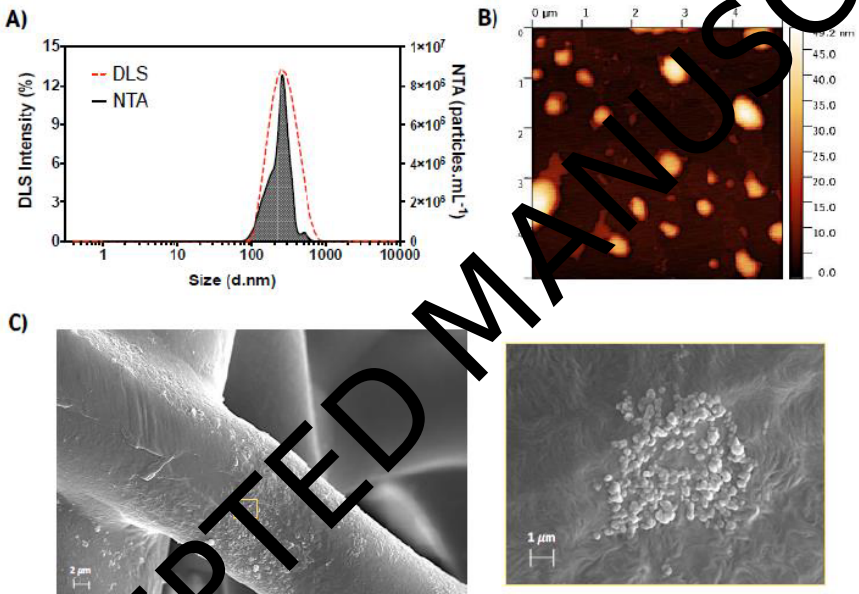

Tables

Table 1. PCL-Nanoparticles physicochemical characterization by Photon Correlation Spectroscopy and Nanoparticle Tracking Analysis measurements.

Samples	Size (nm)	PDI	Zeta Potential (mV)	Encapsulation Efficiency (%)	[NPs] (particles.mL^{-1})
BZC:NPs	277 ± 3	0.10 ± 0.03	-20.1 ± 0.6	93.3 ± 0.9	6 x 10^{12} ± 2 x 10^{10}
NPs	262 ± 7	0.06 ± 0.03	-31.4 ± 0.4	--	1 x 10^{12} ± 5 x 10^{10}

Table 2. Rheological parameters for PL407 hydrogels: viscosity ( ) and sol-gel transition temperature ($T_{sol-gel}$).

Hydrogels	G´ (x10^3, Pa)	G´´ (x10^3, Pa)	G´/G´´	10 °C	32 °C	$T_{sol-gel}$ (°C)
PL	296100	662.9	446.7	390	4714	12.7
PL-NPs	30120	910.8	33.1	39.6	586.1	30.0
PL-BZC	18520	489.8	383.5	1277	2949	< 10
PL-BZC:NPs	113600	296.5	37.8	50.8	1809	20.9